

# 000 001 002 003 004 005 006 007 008 009 010 011 012 013 014 015 016 017 018 019 020 021 022 023 024 025 026 027 028 029 030 031 032 033 034 035 036 037 038 039 040 041 042 043 044 045 046 047 048 049 050 051 052 053 THE END OF MANUAL DECODING: TOWARDS TRULY END-TO-END LANGUAGE MODELS

Anonymous authors

Paper under double-blind review

## ABSTRACT

The “end-to-end” label for LLMs is a misnomer. In practice, they depend on a non-differentiable decoding process that requires laborious, hand-tuning of hyperparameters like temperature and top-p. This paper introduces *AutoDeco*, a novel architecture that enables truly “end-to-end” generation by learning to control its own decoding strategy. We augment the standard transformer with lightweight heads that, at each step, dynamically predict context-specific temperature and top-p values alongside the next-token logits. This approach transforms decoding into a parametric, token-level process, allowing the model to self-regulate its sampling strategy within a single forward pass.

Through extensive experiments on eight benchmarks, we demonstrate that *AutoDeco* not only significantly outperforms default decoding strategies but also achieves performance comparable to an oracle-tuned baseline derived from “hacking the test set”—a practical upper bound for any static method. Besides, we demonstrate an emergent capability for instruction-based decoding control: the model learns to interpret natural language commands (e.g., “generate with low randomness”) and adjusts its predicted temperature and top-p on a token-by-token basis, which may open a new paradigm for steerable and interactive LLM decoding.

## 1 INTRODUCTION

LLMs have become the de-facto standard in NLP, yet the quality of their generated text hinges on a surprisingly manual and heuristic process: the selection of decoding hyperparameters. Parameters like temperature, top-p, and top-k must be carefully chosen through a task-dependent process of manual sweeps and post-hoc filtering (Shi et al., 2024). This not only incurs significant computational and human costs but also profoundly impacts the final output’s creativity, diversity, and factual correctness, undermining the promise of a truly “end-to-end” system.

This reliance on static, hand-tuned parameters creates fundamental bottlenecks. Firstly, the search for an optimal configuration is widely acknowledged as a laborious process because the ideal settings are highly task-dependent; commercial API providers like DeepSeek, for instance, explicitly recommend different temperature settings for distinct application scenarios<sup>1</sup>. However, this problem, runs even deeper: a single static configuration is inherently suboptimal because the ideal level of stochasticity varies dramatically within a single generation. For instance, a model might need high creativity to explore initial reasoning paths but high precision to deliver the final answer. This on-the-fly control is, by design, impossible for current LLMs to achieve natively. Consequently, the prevailing static decoding paradigm is a solution as inefficient as it is ineffective, forcing a one-size-fits-all strategy onto a problem that demands dynamic adaptation.

In this paper, we propose *AutoDeco*, a novel architecture that creates a truly “end-to-end” language model capable of controlling its own decoding process. As illustrated in Figure 1, we augment the standard transformer with lightweight, dedicated prediction heads. At each decoding step, these *AutoDeco* heads leverage the model’s current hidden state to dynamically predict the optimal sampling parameters for the next token. This seamlessly integrates hyperparameter selection into the model’s forward pass, creating a self-regulating inference pipeline that adds nearly-zero latency.

<sup>1</sup>[https://api-docs.deepseek.com/quick\\_start/parameter\\_settings](https://api-docs.deepseek.com/quick_start/parameter_settings)

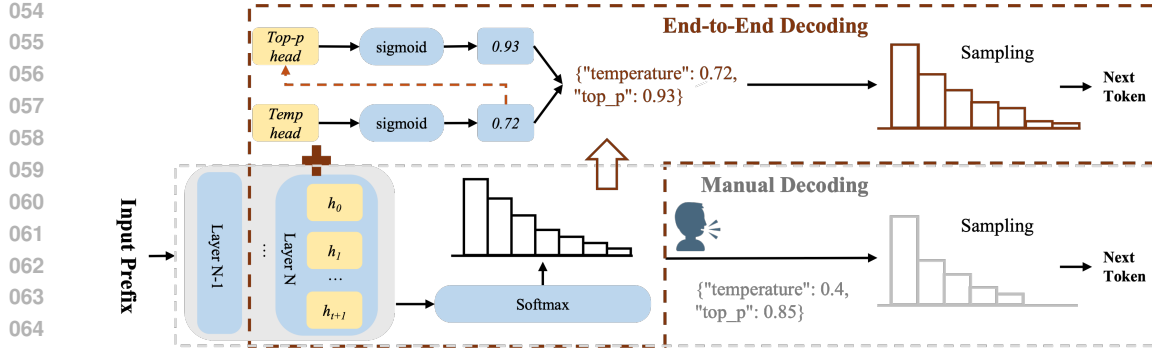


Figure 1: An overview of our proposed end-to-end decoding architecture compared to manual decoding. Our method dynamically predicts temperature and top-p values from the model’s hidden states for each generation step. In contrast, manual decoding (bottom) relies on a single set of static, predefined hyperparameters for the entire sequence generation.

We validate our approach by integrating *AutoDeco* into major model families, including Owen, Llama, GPT, and DeepSeek, requiring only a brief fine-tuning process of 400 steps. Across eight distinct benchmarks, the results are striking: *AutoDeco* not only consistently outperforms standard default decoding settings but also matches or surpasses the performance of meticulously expert-guided tuning (an oracle-tuned baseline derived from “hacking the test set”) hyperparameters. An important secondary benefit of our architecture is the observed capacity for instruction-based decoding control, which is learned unexpectedly during the end-to-end optimization. When prompted with a meta-instruction like, “Please ensure that the diversity of your output is low,” the model immediately responded by lowering its average predicted temperature and top-p values by 0.11 and 0.06, respectively. This demonstrates that *AutoDeco* does not merely automate a tedious process; it endows the model with a new, intuitive way to interpret and act on user intent.

Our contributions are four-fold: **(i)** We propose *AutoDeco*, a novel and lightweight architecture, along with an efficient strategy to train its prediction heads, that makes LLM generation truly “end-to-end” by dynamically predicting decoding parameters at each step. **(ii)** We demonstrate through extensive experiments that *AutoDeco* consistently matches or exceeds the performance of expert-guided tuning, static hyperparameters across eight benchmarks and multiple model families. **(iii)** We demonstrate for the first time that an LLM’s decoding can be controlled by natural language. **(iv)** We release a set of *AutoDeco* heads, trained on the most widely adopted open-source models, providing the community with a streamlined, drop-in solution for immediate deployment.

## 2 AUTODECO

The foregoing discussion raises two fundamental questions that frame the core inquiry of this work:

First, how can we train the *AutoDeco* heads without any token-level “ground-truth” labels for the optimal temperature and top-p values? Second, how can these predictions be integrated into inference without adding computational latency? This section details our solutions to both.

In Section 2.1, we will introduce our training strategy and explain how we train both heads in an “end-to-end” manner. Then, in Section 2.2, we will walk through our inference process. The *AutoDeco* modifies the model’s final output probabilities internally—a design that adds absolutely no extra latency. The result is a model that can be used almost exactly like a standard one, requiring only a “1-line-change” in a user’s code to unlock its dynamic decoding capabilities.

### 2.1 TRAINING STRATEGY

The central challenge in training *AutoDeco* is the absence of token-level “ground-truth” labels for sampling parameters. A natural approach would be to optimize the temperature and top-p heads directly from the final cross-entropy loss of the generated tokens. However, this path is obstructed by the standard top-p sampling algorithm. Its “hard cutoff”—retaining only the smallest set of tokens

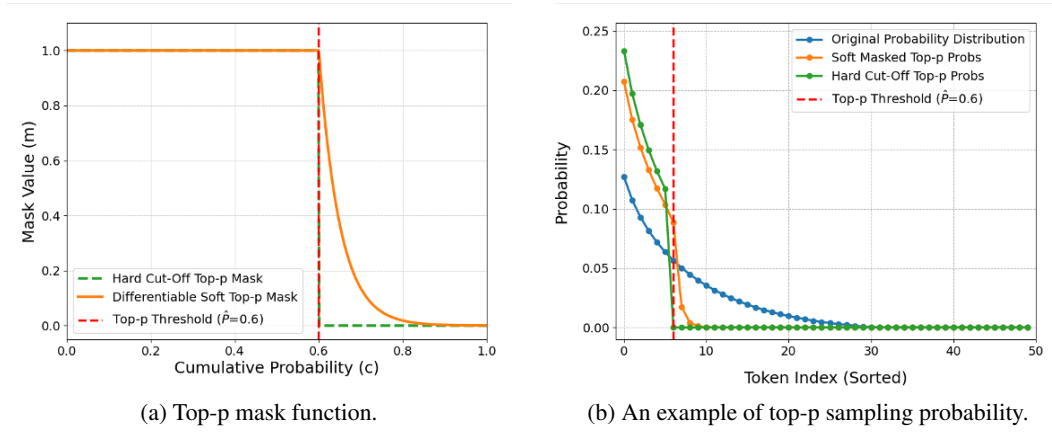


Figure 2: Comparison of the differentiable “soft” top-p sampling (decay steepness  $\alpha = 30$ ) with the standard hard-cutoff method. (a) illustrates the standard hard-cutoff mask, which has a non-differentiable step, against our proposed smooth and differentiable “soft” mask. (b) shows the effect of applying both masks to an example original probability distribution, where the “soft” mask method produces a differentiable probability distribution suitable for “end-to-end” training.

whose cumulative probability exceeds a threshold—is a non-differentiable operation, which severs the gradient flow from the loss back to the top-p head.

To overcome this, we introduce a novel, differentiable “soft” top-p mechanism that is used during training, enabling a fully “end-to-end” optimization strategy. Traditional top-p sampling methods assign a probability of zero to all tokens beyond the top-p threshold, while our approach is different: for tokens that fall outside the top-p threshold, we apply a differentiable weight scaling. The further a token is from the threshold, the more its probability is scaled down, eventually approaching zero.

The following is the training data stream:

1. **Temperature-Scaled Probabilities:** First, we scale the predicted logits  $\mathbf{l}$  to compute the initial probability distribution  $\mathbf{p}$  using the predicted temperature  $\hat{T}$ .

$$\mathbf{p} = \text{softmax} \left( \frac{1}{\hat{T}} \right). \quad (1)$$

2. **Differentiable Mask Generation:** After sorting the probabilities  $\mathbf{p}$  and calculating their cumulative sum  $\mathbf{c}$ , we generate a “soft mask”  $\mathbf{m}^{(\text{sorted})}$ . This is done in a single step that combines the thresholding and decay logic:

$$\mathbf{m}^{(\text{sorted})} = \exp \left( -\alpha \cdot \text{ReLU}(\mathbf{c} - \hat{P}) \right), \quad (2)$$

Here,  $\alpha$  is a hyperparameter that controls the steepness of decay. As shown in Figure 2a, this formulation ensures that for tokens inside the nucleus (where  $\mathbf{c} < \hat{P}$ ), the ReLU term is zero, resulting in a mask value of 1. For tokens outside, the mask value smoothly decays towards zero as their cumulative probability further exceeds  $\hat{P}$ .

3. **Final Probability Distribution:** The “soft mask”  $\mathbf{m}$  (unsorted to match the original vocabulary order) is applied to the initial probabilities, and the result is re-normalized to form the final, differentiable distribution  $\tilde{\mathbf{p}}$ :

$$\tilde{\mathbf{p}} = \frac{\mathbf{p} \odot \mathbf{m}}{\sum(\mathbf{p} \odot \mathbf{m}) + \epsilon}, \quad (3)$$

where  $\epsilon$  is a small constant for numerical stability. In Figure 2b, we provide an example with a vocabulary size of 50 to illustrate how the model’s predicted probability distribution changes after the application of our “soft” top-p sampling. As the probability of the token exceeding  $\hat{P}$  decreases gradually and differentially, the “soft” top-p sampling becomes the final piece of the puzzle for the *AutoDeco*’s “end-to-end” training.

162 **Training.** As the entire process is differentiable, gradients from the standard cross-entropy loss are  
 163 backpropagated to simultaneously update the parameters of both the temperature and top-p heads,  
 164 allowing the model to learn its own optimal, context-specific decoding strategy by directly optimizing  
 165 for the final task objective.

166 Theoretically, these two heads could be trained from the pre-training stage. However, in this paper,  
 167 we build upon a pre-trained LLM, freezing its base parameters and solely training the *AutoDeco*  
 168 heads. While training these heads on SFT data provides a strong baseline, we find that applying some  
 169 certain de-biasing operations to the data can further enhance model performance and robustness:  
 170

- 171 • **Easy-Token Masking.** For many tokens, the base model’s greedy prediction already matches  
 172 the ground-truth. These “easy” tokens often yield an optimal temperature  $\hat{T}_t^*$  near zero, biasing  
 173 the head to be overly conservative. To mitigate this, we randomly mask the training loss for a  
 174 large fraction (e.g., 60%) of these positions, forcing the model to learn from more challenging  
 175 and informative examples.
- 176 • **Dynamic Fine-Tuning.** Conversely, a naive fine-tuning approach can cause the temperature  
 177 head to predict unexpected large values for uncertain tokens. We incorporate Dynamic Fine-  
 178 Tuning (Wu et al., 2025), which re-weights the training loss to focus on tokens where the model  
 179 has a reasonable prior. This teaches the head to apply high temperatures more judiciously in  
 180 situations of calibrated uncertainty, rather than being skewed by outlier signals.

## 181 2.2 INFERENCE: DYNAMIC DECODING

183 At the heart of *AutoDeco* lies a design optimized for efficiency. By seamlessly integrating all dynamic  
 184 adjustments into the model’s standard forward pass, it avoids any separate, costly computational steps.  
 185 This architecture results in a negligible latency overhead, typically adding only 1-2% to the total  
 186 generation time. As illustrated in Figure 1, the process for each token generation step is as follows:  
 187

- 188 1. **Compute Hidden State:** The base LLM computes the final hidden state  $\mathbf{h}_t$ .
- 189 2. **Predict Decoding Parameters:** In parallel, the standard `lm_head` computes the logits while  
 190 the *AutoDeco* heads predict the dynamic parameters. The temperature is predicted directly from  
 191 the hidden state. Crucially, the top-p head then uses both the hidden state *and* the just-predicted  
 192 temperature as input:

$$193 \hat{T}_t = \text{temp\_head}(\mathbf{h}_t), \quad \hat{P}_t = \text{top-p\_head}(\mathbf{h}_t, \hat{T}_t). \quad (4)$$

194 This micro-dependency, shown as a dashed arrow in Figure 1, allows for a more nuanced  
 195 interplay between the two parameters.

- 196 3. **Internal Probability Modification:** The model immediately uses the predicted  $\hat{T}_t$  and  $\hat{P}_t$  to  
 197 internally rescale and filter the logits, producing a final, dynamically-adjusted distribution.

199 **Latency and Simplicity.** The *AutoDeco* heads (simple 2-layer MLPs) add negligible computational  
 200 overhead compared to the massive transformer layers. This internal architecture results in only 1-2%  
 201 additional latency and makes usage incredibly simple, and ensures seamless integration, allowing an  
 202 *AutoDeco*-enabled model to serve as a drop-in replacement for its standard counterpart, requiring no  
 203 modifications to the user’s existing generation logic.

## 205 3 EXPERIMENTS

207 We conduct extensive experiments to validate *AutoDeco*, structuring our evaluation around its core  
 208 contributions to performance, efficiency, and a surprising capability that emerged as a byproduct.  
 209

- 210 • In Section 3.2.1, we demonstrate the superior performance of *AutoDeco*. It not only substantially  
 211 outperforms standard, non-expert decoding baselines (Greedy Search and Default Sampling)  
 212 but also matches or even slightly surpasses the performance of optimal static hyperparameters  
 213 found through an exhaustive expert-guided tuning.
- 214 • Following this, in Section 3.2.2, we analyze its practical efficiency and confirm that *AutoDeco*  
 215 introduces a minimal computational burden, with a marginal latency increase of 1-2% and a  
 negligible memory footprint.

216 • A noteworthy finding is presented in Section 3.3: the emergent capability of AutoDeco to  
 217 interpret natural language commands to dynamically steer its own generation style. This  
 218 development is a significant step towards more intuitive and controllable AI.  
 219

220 **3.1 EXPERIMENTAL SETUP**  
 221

222 **Models.** To demonstrate broad applicability, we select representative models from three of the most  
 223 popular open-source model families. All *AutoDeco* heads are trained on top of the official pre-trained  
 224 checkpoints of these models:

225 • **Llama-3.1-Nemotron-Nano-8B-v1**(Bercovich et al., 2025): A general-purpose model from the  
 226 widely-used Llama family, developed by Nvidia (hereinafter Llama-Nemotron-8B).  
 227 • **R1-Distill-Qwen-7B**(Guo et al., 2025): A distilled model from the Qwen family developed by  
 228 DeepSeek, known for its strong reasoning capabilities.  
 229 • **Qwen3-30B-A3B-Instruct-2507**(QwenTeam, 2025): An advanced MoE architecture instruct  
 230 (non-thinking) model from Qwen. (hereinafter Qwen3-30B-Instruct)  
 231 • **Qwen3-235B-A22B-Thinking-2507**(QwenTeam, 2025): An advanced MoE architecture Thinking  
 232 model from Qwen. (hereinafter Qwen3-235B-Thinking)  
 233 • **OpenAI-GPT-OSS-20B**(Agarwal et al., 2025): A MoE model with 20B parameters released by  
 234 OpenAI. The reasoning effort is set to medium by default.  
 235

236 More models, including **DeepSeek-V3.1-Terminus (with multi-token prediction)** (DeepSeek-AI,  
 237 2024), and results can be found in the Appendix 9.

239 **Datasets.** The models are trained on a focused domain and evaluated on a wide range of tasks to  
 240 test for generalization.  
 241

242 • **Training Data:** The *AutoDeco* heads are trained on a specialized dataset of reject sampling  
 243 trajectories. These trajectories were generated by sampling solutions from our four base models  
 244 on problems from the DeepMath-103K dataset (He et al., 2025).  
 245 • **Evaluation Benchmarks:** We evaluate on a diverse suite of eight benchmarks, split into two  
 246 categories to assess both in-domain and out-of-domain performance:  
 247 – **In-Domain (Math):** AIME (24+25), BRUMO25, HMMT25 (Balunović et al., 2025), and  
 248 BeyondAIME (ByteDance-Seed, 2025).<sup>2</sup>  
 249 – **Out-of-Domain (General Tasks):** GPQA-Diamond (Rein et al., 2024) and MMLU-Pro  
 250 (Wang et al., 2024b) (QA) , LiveCodeBenchV6 (Jain et al., 2024) (Code), and IFEval (Zhou  
 251 et al., 2023) (Instruction Following).

252 **Baselines and Evaluation.** We evaluate *AutoDeco* against two standard, non-expert decoding  
 253 strategies: **Greedy Search** and **Default Sampling** ( $\hat{T} = 1.0$ ,  $\hat{P} = 1.0$ ). Furthermore, to establish a  
 254 practical upper bound, we also compare against an **Expert-Guided Tuning**. It is crucial to note that  
 255 this expert-tuned baseline is an *oracle* setting, as it involves finding the optimal static hyperparameters  
 256 by tuning on the test set—a process that is infeasible in real-world applications.  
 257

258 Our primary metric is Pass@1 accuracy, estimated via oversampling with 128 samples per problem  
 259 (with 8 random seeds, 16 samples per seed). The maximum generation length is set to 32768.  
 260

261 **3.2 MAIN RESULTS**  
 262

263 We present our main findings separately for mathematical reasoning and open-domain question  
 264 answering to provide a clear and detailed view of *AutoDeco*’s performance across different domains.  
 265

266 **3.2.1 PERFORMANCE**  
 267

268 **In-Domain Performance.** As shown in Table 1 *AutoDeco* consistently demonstrates a performance  
 269 boost compared to Greedy Search and Default Sampling. For instance, on Llama-Nemotron-8B, it

<sup>2</sup>We focus on these recent, hard benchmarks to mitigate the risk of data leakage issues in older datasets.

Table 1: Pass@1 accuracy on mathematical reasoning benchmarks. *AutoDeco* consistently outperforms both Greedy Search and Default Sampling methods across various models.

Model	Method	AIME	BRUMO25	HMMT25	BeyondAIME	Average
Llama-Nemotron-8B	Greedy Search	51.67	56.67	26.67	<b>35.00</b>	42.50
	Default Sampling	50.84±1.44	57.89±1.46	29.82±1.60	31.82±0.40	42.59
	<i>AutoDeco</i> (Ours)	<b>55.43±1.22</b>	<b>60.60±0.98</b>	<b>33.98±1.14</b>	34.19±0.65	<b>46.05</b>
R1-Distill-Qwen-7B	Greedy Search	38.33	43.33	16.67	24.00	30.58
	Default Sampling	43.49±1.38	49.01±1.10	22.32±0.83	24.21±0.79	34.76
	<i>AutoDeco</i> (Ours)	<b>47.03±1.12</b>	<b>51.64±1.05</b>	<b>24.14±0.39</b>	<b>26.65±0.49</b>	<b>37.37</b>
Qwen3-30B-Instruct	Greedy Search	65.00	63.33	36.67	44.00	52.25
	Default Sampling	67.92±1.36	66.02±1.11	<b>43.88±1.28</b>	46.38±0.47	56.05
	<i>AutoDeco</i> (Ours)	<b>68.46±0.76</b>	<b>67.21±0.87</b>	43.73±1.26	<b>46.75±0.18</b>	<b>56.54</b>
Qwen3-235B-Thinking	Greedy Search	80.00	79.92	63.33	51.00	68.56
	Default Sampling	80.76±0.43	79.32±0.79	61.95±0.94	49.15±0.33	67.80
	<i>AutoDeco</i> (Ours)	<b>82.79±0.72</b>	<b>80.96±1.05</b>	<b>64.17±0.91</b>	<b>51.19±0.47</b>	<b>69.78</b>
OpenAI-GPT-OSS-20B	Greedy Search	56.67	66.67	<b>46.67</b>	36.00	51.50
	Default Sampling	69.61±1.32	67.03±1.12	44.24±2.28	45.69±0.13	56.64
	<i>AutoDeco</i> (Ours)	<b>72.33±1.20</b>	<b>68.25±0.58</b>	46.21±1.08	<b>45.72±0.44</b>	<b>58.13</b>

Table 2: Pass@1 accuracy on general-domain benchmarks. *AutoDeco* shows exciting generalization performance across General QA, Code Generation, and Instruction Following tasks.

Model	Method	GPQA-Diamond	MMLU-Pro	LiveCodeBenchV6	IFEval	Average
Llama-Nemotron-8B	Greedy Search	<b>51.01</b>	52.00	19.17	<b>71.53</b>	48.43
	Default Sampling	44.93	54.00	21.22	65.25	46.35
	<i>AutoDeco</i> (Ours)	50.52	<b>55.64</b>	<b>21.68</b>	71.02	<b>49.72</b>
R1-Distill-Qwen-7B	Greedy Search	37.87	47.20	49.13	32.90	39.32
	Default Sampling	47.41	47.65	53.00	32.35	42.47
	<i>AutoDeco</i> (Ours)	<b>48.91</b>	<b>50.75</b>	<b>53.14</b>	<b>33.90</b>	<b>46.88</b>
Qwen3-30B-Instruct	Greedy Search	65.86	78.00	47.75	<b>83.73</b>	68.84
	Default Sampling	69.82	76.25	48.52	81.52	69.03
	<i>AutoDeco</i> (Ours)	<b>69.96</b>	<b>78.38</b>	<b>49.80</b>	82.81	<b>70.24</b>
Qwen3-235B-Thinking	Greedy Search	77.78	<b>81.00</b>	77.25	31.98	67.00
	Default Sampling	80.81	80.33	77.47	31.61	67.56
	<i>AutoDeco</i> (Ours)	<b>81.13</b>	79.20	<b>78.10</b>	<b>32.90</b>	<b>67.83</b>
OpenAI-GPT OSS-20B	Greedy Search	59.60	67.00	69.69	29.94	56.56
	Default Sampling	65.67	68.00	70.15	30.68	58.63
	<i>AutoDeco</i> (Ours)	<b>66.48</b>	<b>69.12</b>	<b>71.25</b>	<b>30.84</b>	<b>59.42</b>

achieves an average score of 46.05, a substantial improvement of nearly 3.5 absolute points over Default Sampling and Greedy Search.

One may notice that the performance gain from *AutoDeco* is less pronounced on Qwen3-30B-A3B-Instruct-2507 compared to other models. This may stem from Qwen3-30B-A3B-Instruct-2507, as a non-thinking-model, produces answers that are significantly shorter than the other models. Consequently, the sensitivity of task accuracy to variations in sampling parameters is substantially lower, a trend that is further demonstrated by the results in Table 2.

**Out-of-Domain Generalization.** More strikingly, despite being trained exclusively on mathematical reasoning, *AutoDeco* demonstrates powerful zero-shot generalization to a diverse set of out-of-domain tasks (Table 2). It consistently secures the highest average scores across general QA, code generation, and instruction following. This strong performance reveals two interesting patterns.

First, the magnitude of improvement is remarkably consistent across domains. For example, on R1-Distill-Qwen-7B, *AutoDeco* improves the average score on general tasks by 4.4 points over Default Sampling—a gain even surpassing that seen in the math domain. This suggests that the benefits of dynamic decoding are fundamental and not tied to a specific task type.

Second, *AutoDeco* shows an ability to dynamically balance deterministic and stochastic strategies. On general tasks, Default Sampling is not always better than Greedy Search (e.g., on Llama-Nemotron-8B for GPOA-Diamond and IFFEval). In these cases, *AutoDeco* learns to predict more deterministic,

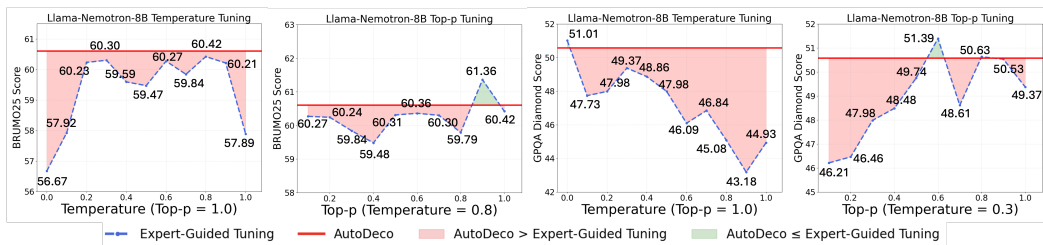
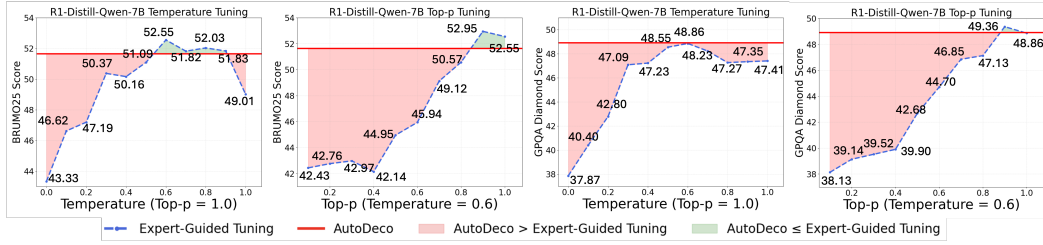
(a) Llama-Nemotron-8B with *AutoDeco*.(b) R1-Distill-Qwen-7B with *AutoDeco*.

Figure 3: Expert-Guided Tuning Comparison with Search Interval of 0.1. Temperature is adjusted first (setting top-p to 1.0), and the selection is made based on the best performance of temperature to conduct the search for top-p. *AutoDeco* achieves competitive performance without requiring any prior empirical tuning or domain-specific expert knowledge.

Table 3: Pass@64 accuracy on mathematical reasoning benchmarks. Comparing Default Sampling with the *AutoDeco* method.

Model	Method	AIME	BRUMO25	HMMT25	BeyondAIME	Average
Llama-Nemotron-8B	Default Sampling	83.31	88.70	88.70	88.70	87.35
	<i>AutoDeco</i> (Ours)	<b>87.72</b>	<b>90.42</b>	<b>90.42</b>	<b>90.42</b>	<b>89.75</b>
R1-Distill-Qwen-7B	Default Sampling	76.89	79.95	62.94	63.90	70.92
	<i>AutoDeco</i> (Ours)	<b>80.36</b>	<b>82.48</b>	<b>71.44</b>	<b>64.84</b>	<b>74.78</b>
Qwen3-30B-Instruct	Default Sampling	90.98	92.20	71.07	77.50	82.94
	<i>AutoDeco</i> (Ours)	<b>92.06</b>	<b>93.11</b>	<b>71.70</b>	<b>77.58</b>	<b>83.61</b>
Qwen3-235B-Thiking	Default Sampling	91.67	95.00	<b>88.19</b>	71.00	86.47
	<i>AutoDeco</i> (Ours)	<b>92.50</b>	<b>98.24</b>	87.50	<b>71.00</b>	<b>87.31</b>
OpenAI-GPT-OSS-20B	Default Sampling	93.96	94.99	84.54	<b>85.24</b>	89.68
	<i>AutoDeco</i> (Ours)	<b>95.17</b>	<b>96.67</b>	<b>90.36</b>	84.00	<b>91.55</b>

low-temperature parameters, allowing it to match or exceed the performance of the stronger greedy baseline. Conversely, when stochasticity is beneficial, it raises the temperature to outperform Default Sampling.

The above findings suggest that *AutoDeco* is not simply learning “what” to generate, but rather the fundamental “meta-skill of how” to generate text effectively. By training on a high-signal domain like mathematics, it learns universal principles for balancing exploration and exploitation. We also show that *AutoDeco* has the ability to adapt to different task requirements (Stability vs. Creativity) in Appendix 9. We will further discuss this in Sec. 3.3, and this finding challenges the conventional assumption that adaptive decoding requires broad, task-matched supervision, and instead points toward a more efficient, modular paradigm for real “end-to-end” controllable generation.

**Pass@ $k$  Performance.** Some recent works (Yue et al., 2025; Chen et al., 2025) have highlighted a potential trade-off in the training of reasoning models, where achieving superb pass@1 accuracy can come at the expense of performance on pass@ $k$  (for  $k > 1$ ). To investigate this, we present an extended evaluation of our method on pass@ $k$  ( $k = 16, 32, 64$ ) accuracies.

378 With encouraging results, we find that the absolute improvements delivered by *AutoDeco* at higher  
 379  $k$ -values are consistent with, and at times even slightly greater than, those observed at pass@1. We  
 380 show pass@64 in Table 3, and for other results, please refer to the Appendix 9.  
 381

382 It is important to note that for any given model, pass@ $k$  accuracy is inherently much higher than  
 383 pass@1 accuracy. Consequently, it is obvious that securing absolute performance gains becomes  
 384 substantially more difficult, and a similar absolute improvement at pass@64 translates to a much  
 385 larger relative error reduction, compared to pass@1. For example, on the OpenAI-GPT-OSS-20B  
 386 model, we observe that the performance gains from *AutoDeco* are consistent across different  $k$  values  
 387 in pass@ $k$  evaluations. More importantly, this consistent absolute gain translates to a significantly  
 388 larger impact in higher-accuracy (when  $k$  is large) scenarios. The relative error reduction dramatically  
 389 increases from **3.5%** at pass@1 to **18.1%** at pass@64. This demonstrates that as the task becomes  
 390 easier for the baseline model (i.e., the error rate decreases at high  $k$ ), the performance gains from our  
 391 method become even more significant.  
 392

393 **Comparison with Expert-Guided Tuning.** In real-world applications, developers often undertake  
 394 a laborious tuning process to find task-specific, optimal static hyperparameters. To assess how  
 395 *AutoDeco* compares to this best-case scenario, we simulate an expert with an unfair advantage: access  
 396 to a test-set oracle. As shown in Figure 3, we first perform a fine-grained search to find the optimal  
 397 static temperature on the test set, and then, using that temperature, find the optimal top-p. This  
 398 process represents the practical upper bound for any static decoding strategy.  
 399

400 The results are striking. *AutoDeco*’s single-pass performance is nearly identical to this oracle-tuned  
 401 baseline, with the performance gap consistently less than one point across all models and datasets.  
 402 Given that the Expert-Guided Tuning relies on “hacking the test set”, a process impossible in any  
 403 real-world scenario where the test data is unknown, we can confidently assert that *AutoDeco* is  
 404 effectively superior to any feasible expert-tuning strategy in practice.  
 405

406 Furthermore, the figure highlights the fundamental limitation of static decoding: the optimal hyper-  
 407 parameters are extremely task-dependent. For instance, Llama-Nemotron-8B requires drastically  
 408 different settings for BRUMO25 ( $\hat{T} = 0.8, \hat{P} = 0.9$ ) versus GPQA-Diamond ( $\hat{T} = 0.3, \hat{P} = 0.6$ ).  
 409 However, in real-world scenarios, a model developer has no way to switch hyperparameters based on  
 410 the user’s query type. *AutoDeco* elegantly solves this problem. By achieving near-oracle performance  
 411 automatically and on-the-fly for any task, it provides the optimal and, frankly, only practical solution  
 412 for developers seeking robust, high-performance generation across diverse user inputs.  
 413

414 **Compatibility with Advanced Decoding Algorithms.** In practice, using only the model for next-  
 415 token prediction might be inefficient. For industrial and production-level deployment and usage,  
 416 speculative decoding is a very common and advanced technique, such as multi-token prediction  
 417 (MTP) (DeepSeek-AI, 2024) that is widely used in the state-of-the-art models of various families  
 418 (QwenTeam, 2025). Our *AutoDeco* is fully compatible with speculative decoding mechanisms:  
 419

- 420 • Theoretically, speculative decoding (such as MTP, which is currently applied in production-level  
 421 models like DeepSeek-V3.1, Qwen3-Next) is fundamentally still of the form of autoregression.  
 422 Sampling parameters such as Temperature and Top-p are widely and continuously employed  
 423 within the speculative decoding framework to control the diversity and quality of the final  
 424 accepted tokens.
- 425 • To empirically confirm this seamless integration, we conducted a MTP experiment on the  
 426 advanced LLM DeepSeek-V3.1-Terminus. It shows that our method does not require any  
 427 specific adaptation and will not break the process of speculative decoding. (Please refer to  
 428 Appendix 9 for detailed results.)

429 **Ablation Study.** A natural question is what role the temperature and top-p heads play individually.  
 430 To isolate their effects, we evaluate on AIME using R1-Distill-Qwen-7B to conduct an ablation study,  
 431 with the results presented in Figure 4. The most striking finding is the remarkable effectiveness of  
 432 each component in isolation. Using either the temperature head or the top-p head alone achieves an  
 433 average performance gain of approximately 3-3.5 absolute points over the Default Sampling baseline.  
 434

432 Table 4: FLOPs, Memory Usage and latency (1k tokens) across various prompt length for R1-Distill-  
 433 Qwen-7B with/without temp head and top-p head.

Metrics	Method	1k	2k	4k	8k	16k	24k
FLOPs	Default Sampling	2.89e+13	4.34e+13	7.23e+13	13.03e+13	24.61e+13	36.19e+13
	<i>AutoDeco</i> (Ours)	2.89e+13	4.34e+13	7.24e+13	13.03e+13	24.62e+13	36.20e+13
Latency (s)	Default Sampling	18.23	18.86	18.93	19.72	22.11	25.76
	<i>AutoDeco</i> (Ours)	18.84	19.10	19.43	20.03	22.36	26.05
Memory (MB)	Default Sampling	15546	16032	17130	19098	23182	27262
	<i>AutoDeco</i> (Ours)	15550	16036	17134	19102	23183	27266

443 This result is highly significant. It demonstrates that sub-  
 444 substantial improvements in decoding do not require a sophis-  
 445 ticated architecture. A single, lightweight prediction head  
 446 is sufficient to dramatically outperform standard static  
 447 decoding methods.

448 Of course, while each head is powerful on its own, our  
 449 results also confirm that the full *AutoDeco* model, with  
 450 both heads, yields the best performance. They provide  
 451 complementary benefits, allowing for even finer-grained  
 452 control over the generation process to achieve optimal  
 453 results.

### 455 3.2.2 EFFICIENCY

456 A critical advantage of *AutoDeco* is its computational efficiency. To quantify this, we evaluated its  
 457 overhead against Default Sampling across three key metrics, with results summarized in Table 4.

458 The analysis shows that the additional computational burden is minimal. The FLOPs are virtually  
 459 identical to the baseline, and the memory footprint increases by a mere 4 MB, an insignificant amount  
 460 for modern hardware. The impact on latency is also negligible. This overhead remains consistently  
 461 low regardless of prompt length, adding a consistent overhead of 0.29-0.6 s/k tokens, which translates  
 462 to an average relative increase of just 1.7%.

463 These results empirically validate that *AutoDeco* is a lightweight enhancement. When considering  
 464 the substantial performance gains and the convenience of automatic, task-agnostic hyperparameter  
 465 tuning demonstrated in Sec. 3.2.1, this minor computational cost becomes trivial. *AutoDeco* thus  
 466 presents a highly practical solution, offering significant benefits for a negligible price.

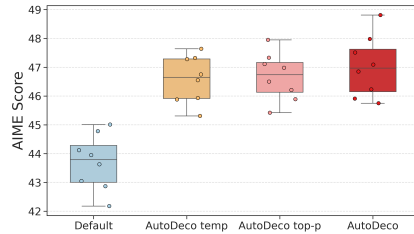
467 The analysis regarding training efficiency can be found in the Appendix 8.

### 470 3.3 EMERGENT CONTROL OF DECODING VIA NATURAL LANGUAGE

471 Beyond outperforming static methods, we observe that *AutoDeco* acquires a crucial capability: it  
 472 learns to map abstract, high-level commands (such as instructions for diversity or certainty) directly  
 473 to its internal decoding parameters. This learned instruction-based control enables the model to  
 474 dynamically respond to user intent regarding the desired generation style, marking a significant  
 475 step towards truly end-to-end and controllable generation. For this phenomenon, we conducted an  
 476 in-depth evaluation and discussion, which are detailed in the Appendix 7.

## 478 4 RELATED WORKS

481 The process of generating text from a language model, known as decoding, is a critical step that  
 482 significantly influences the quality of the output(Wang et al., 2025; Shi et al., 2024). One directly  
 483 related work is Adaptive Decoding (Dhuliawala et al., 2024), which also introduces a learned decoding  
 484 head. Their method focuses on predicting temperature and utilizes reinforcement learning (RL) for  
 485 training. Our work differs in two main aspects: 1) we learn to control both temperature and top-p,  
 486 and 2) we employ a fully differentiable pipeline that allows for direct end-to-end training from the



487 Figure 4: Ablation study on *AutoDeco* architecture designs. Joint optimization achieves the highest AIME Score.

486 next-token prediction loss, instead of RL. The Other Existing decoding strategies can be broadly  
 487 categorized into deterministic, stochastic sampling, and model-based approaches, most of which  
 488 traditionally rely on static, predefined configurations.

489 **Deterministic Decoding.** Deterministic methods produce a single, reproducible output for a given  
 490 input. The most fundamental of these is Greedy Search, which selects the token with the highest  
 491 probability at each step. Another classic one is beam search, which maintains a “beam” of  $k$  most  
 492 probable partial sequences to explore a larger search space (Sutskever et al., 2014; Graves, 2013).  
 493 However, both of them are known to favor dull, high-frequency phrases (Vijayakumar et al., 2016),  
 494 this results in their good performance on Machine Translation and QA tasks, but not suitable for  
 495 open-ended generation tasks. A more recent line of deterministic methods, Contrastive Search(Su &  
 496 Collier, 2022; Su et al., 2022), directly optimizes for open-ended generation quality by penalizing  
 497 tokens that are too similar to previous tokens, effectively mitigating the degeneration problem.

498 **Stochastic Sampling.** To inject diversity, stochastic sampling methods are essential. These methods  
 499 sample from the model’s output probability distribution, which is typically modulated by some  
 500 hyperparameters. However, unrestricted sampling can produce incoherent text. To counter this,  
 501 truncation methods were developed. Top-K sampling(Fan et al., 2018) restricts the sampling pool  
 502 to the  $k$  most likely tokens, while the more adaptive Nucleus Sampling (top-p)(Holtzman et al.)  
 503 selects the smallest set of tokens whose cumulative probability exceeds a threshold  $p$ . Despite their  
 504 power, as our introduction highlights, finding the optimal configuration for these hyperparameters is  
 505 a non-trivial, task-dependent manual process (Shi et al., 2024).

506 **Model-Based Decoding.** To gain more fine-grained control over generation, a third category  
 507 of methods modifies the model’s output distribution using external signals or auxiliary models.  
 508 Early examples include **Plug-and-Play Language Models**, which leverage attribute models to  
 509 steer generation towards desired topics (Dathathri et al.). More recently, **Contrastive Decoding**  
 510 uses a smaller “amateur” model to steer a larger “expert” model away from generic text (Li et al.,  
 511 2023; Chuang et al., 2023). Similarly, Speculative Decoding utilizes a faster “draft” model to  
 512 generate sequences of tokens that are then verified by the larger model, significantly accelerating  
 513 inference (Leviathan et al., 2023; Chen et al., 2023). There is also an art to verification methods (Liu  
 514 et al., 2025). While they are effective, they still operate under a fixed algorithmic framework: the  
 515 choice of the “guidance model” itself acts as another form of hyperparameter. For example, in  
 516 contrastive decoding and speculative decoding, the authors suggest that using a smaller LM of the  
 517 same architecture as the guidance model yields the best results.

518 Despite this rich landscape of research, a fundamental limitation persists: all these methods rely  
 519 on a static decoding strategy. Whether it’s a fixed algorithm (like Beam Search) or a fixed set of  
 520 hyperparameters, this “one-size-fits-all” approach is inherently suboptimal. In contrast, *AutoDeco*  
 521 proposes a paradigm shift. Instead of relying on fixed hyperparameters or predefined heuristics, we  
 522 empower the model to dynamically control its own stochasticity at each generation step.

## 524 5 CONCLUSION AND FUTURE WORK

525 In this work, we challenged that the “end-to-end” label for LLM is a misnomer. We introduced  
 526 *AutoDeco*, a truly “end-to-end” architecture that empowers models to dynamically control their  
 527 own decoding strategy. By learning to predict token-level temperature and top-p values, *AutoDeco*  
 528 transforms decoding from a manual, static process into a dynamic, self-regulating pipeline.

529 Our extensive experiments reveal three key contributions. First, *AutoDeco* demonstrates remarkable  
 530 generalization, consistently outperforming standard decoding methods across diverse models  
 531 and tasks, even matching oracle-tuned baselines without any task-specific tuning. Second, this  
 532 performance is achieved with negligible computational overhead, making it a practical, drop-in  
 533 enhancement for any transformer-based model. Additionally, we discovered an intriguing emergent  
 534 capability: *AutoDeco* learns to interpret natural language commands to steer its own generation style,  
 535 a foundational step towards more intuitive human-AI interaction.

536 Future Work. Our immediate future work involves jointly training the base model with *AutoDeco*. We  
 537 believe this will address current limitations like imprecise prompt-based control and data biases—both  
 538 likely consequences of a frozen backbone—thereby enabling more granular control over generation.

540 STATEMENTS

541

542 ETHICS STATEMENT

543

544 The authors of this paper have read and agree to abide by the ICLR Code of Ethics. We believe that  
 545 this work does not raise any significant ethical concerns. Our research did not involve experiments  
 546 with human subjects, nor did it process sensitive personal data. All datasets used in our study are  
 547 publicly available. We foresee no direct negative societal impacts from the methods and potential  
 548 applications presented in this work.

549

550 REPRODUCIBILITY STATEMENT

551

552 We are committed to ensuring the reproducibility of our research. We have provided comprehensive  
 553 experimental details in the main paper and Appendix 6, including dataset preprocessing proce-  
 554 dures, model architecture specifications, full training details, and all hyperparameter configura-  
 555 tions. Furthermore, we will make our source code and model checkpoints publicly available.

556

557 REFERENCES

558 Sandhini Agarwal, Lama Ahmad, Jason Ai, Sam Altman, Andy Applebaum, Edwin Arbus, Rahul K  
 559 Arora, Yu Bai, Bowen Baker, Haiming Bao, et al. gpt-oss-120b & gpt-oss-20b model card. *arXiv*  
 560 *preprint arXiv:2508.10925*, 2025.

561

562 Mislav Balunović, Jasper Dekoninck, Ivo Petrov, Nikola Jovanović, and Martin Vechev. Math-  
 563 arena: Evaluating llms on uncontaminated math competitions, February 2025. URL <https://matharena.ai/>.

564

565 Akhiad Bercovich, Itay Levy, Izik Golan, Mohammad Dabbah, Ran El-Yaniv, Omri Puny, Ido Galil,  
 566 Zach Moshe, Tomer Ronen, Najeeb Nabwani, et al. Llama-nemotron: Efficient reasoning models.  
 567 *arXiv preprint arXiv:2505.00949*, 2025.

568

569 ByteDance-Seed. Beyondaime: Advancing math reasoning evaluation beyond high school olympiads.  
 570 <https://huggingface.co/datasets/ByteDance-Seed/BeyondAIME>, 2025.

571

572 Charlie Chen, Sebastian Borgeaud, Geoffrey Irving, Jean-Baptiste Lespiau, Laurent Sifre, and John  
 573 Jumper. Accelerating large language model decoding with speculative sampling. *arXiv preprint*  
 574 *arXiv:2302.01318*, 2023.

575

576 Zhipeng Chen, Xiaobo Qin, Youbin Wu, Yue Ling, Qinghao Ye, Wayne Xin Zhao, and Guang Shi.  
 577 Pass@k training for adaptively balancing exploration and exploitation of large reasoning models,  
 578 2025. URL <https://arxiv.org/abs/2508.10751>.

579

580 Yung-Sung Chuang, Yujia Xie, Hongyin Luo, Yoon Kim, James R Glass, and Pengcheng He. Dola:  
 581 Decoding by contrasting layers improves factuality in large language models. In *The Twelfth  
 582 International Conference on Learning Representations*, 2023.

583

584 Sumanth Dathathri, Andrea Madotto, Janice Lan, Jane Hung, Eric Frank, Piero Molino, Jason  
 585 Yosinski, and Rosanne Liu. Plug and play language models: A simple approach to controlled text  
 586 generation. In *International Conference on Learning Representations*.

587

588 DeepSeek-AI. Deepseek-v3 technical report, 2024. URL <https://arxiv.org/abs/2412.19437>.

589

590 Shehzaad Dhuliawala, Ilia Kulikov, Ping Yu, Asli Celikyilmaz, Jason Weston, Sainbayar Sukhbaatar,  
 591 and Jack Lanchantin. Adaptive decoding via latent preference optimization. *arXiv preprint*  
 592 *arXiv:2411.09661*, 2024.

593

594 Angela Fan, Mike Lewis, and Yann Dauphin. Hierarchical neural story generation. In *Proceedings  
 595 of the 56th Annual Meeting of the Association for Computational Linguistics (Volume 1: Long  
 596 Papers)*, pp. 889–898, 2018.

594 Alex Graves. Generating sequences with recurrent neural networks. *arXiv preprint arXiv:1308.0850*,  
 595 2013.

596

597 Daya Guo, Dejian Yang, Haowei Zhang, Junxiao Song, Ruoyu Zhang, Runxin Xu, Qihao Zhu,  
 598 Shirong Ma, Peiyi Wang, Xiao Bi, et al. Deepseek-r1: Incentivizing reasoning capability in llms  
 599 via reinforcement learning. *arXiv preprint arXiv:2501.12948*, 2025.

600 Zhiwei He, Tian Liang, Jiahao Xu, Qiuwei Liu, Xingyu Chen, Yue Wang, Linfeng Song, Dian  
 601 Yu, Zhenwen Liang, Wenxuan Wang, et al. Deepmath-103k: A large-scale, challenging, de-  
 602 contaminated, and verifiable mathematical dataset for advancing reasoning. *arXiv preprint*  
 603 *arXiv:2504.11456*, 2025.

604 Ari Holtzman, Jan Buys, Li Du, Maxwell Forbes, and Yejin Choi. The curious case of neural text  
 605 degeneration. In *International Conference on Learning Representations*.

606

607 Naman Jain, King Han, Alex Gu, Wen-Ding Li, Fanjia Yan, Tianjun Zhang, Sida Wang, Armando  
 608 Solar-Lezama, Koushik Sen, and Ion Stoica. Livecodebench: Holistic and contamination free  
 609 evaluation of large language models for code. *arXiv preprint*, 2024.

610 Yaniv Leviathan, Matan Kalman, and Yossi Matias. Fast inference from transformers via speculative  
 611 decoding. In *International Conference on Machine Learning*, pp. 19274–19286. PMLR, 2023.

612

613 Xiang Lisa Li, Ari Holtzman, Daniel Fried, Percy Liang, Jason Eisner, Tatsunori Hashimoto, Luke  
 614 Zettlemoyer, and Mike Lewis. Contrastive decoding: Open-ended text generation as optimization.  
 615 In *The 61st Annual Meeting Of The Association For Computational Linguistics*, 2023.

616 Xiaoyuan Liu, Tian Liang, Zhiwei He, Jiahao Xu, Wenxuan Wang, Pinjia He, Zhaopeng Tu, Haitao  
 617 Mi, and Dong Yu. Trust, but verify: A self-verification approach to reinforcement learning with  
 618 verifiable rewards. 2025. URL <https://arxiv.org/abs/2505.13445>.

619

620 QwenTeam. Qwen3 technical report, 2025. URL <https://arxiv.org/abs/2505.09388>.

621

622 David Rein, Betty Li Hou, Asa Cooper Stickland, Jackson Petty, Richard Yuanzhe Pang, Julien  
 623 Dirani, Julian Michael, and Samuel R. Bowman. GPQA: A graduate-level google-proof q&a  
 624 benchmark. In *First Conference on Language Modeling*, 2024. URL <https://openreview.net/forum?id=Ti67584b98>.

625

626 Chufan Shi, Haoran Yang, Deng Cai, Zhisong Zhang, Yifan Wang, Yujiu Yang, and Wai Lam. A  
 627 thorough examination of decoding methods in the era of llms. *arXiv preprint arXiv:2402.06925*,  
 628 2024.

629

630 Yixuan Su and Nigel Collier. Contrastive search is what you need for neural text generation. *arXiv  
 preprint arXiv:2210.14140*, 2022.

631

632 Yixuan Su, Tian Lan, Yan Wang, Dani Yogatama, Lingpeng Kong, and Nigel Collier. A contrastive  
 633 framework for neural text generation. *Advances in Neural Information Processing Systems*, 35:  
 634 21548–21561, 2022.

635

636 Ilya Sutskever, Oriol Vinyals, and Quoc V Le. Sequence to sequence learning with neural networks.  
*Advances in neural information processing systems*, 27, 2014.

637

638 Ashwin K Vijayakumar, Michael Cogswell, Ramprasad R Selvaraju, Qing Sun, Stefan Lee, David  
 639 Crandall, and Dhruv Batra. Diverse beam search: Decoding diverse solutions from neural sequence  
 640 models. *arXiv preprint arXiv:1610.02424*, 2016.

641

642 Haoran Wang, Xiongxiao Xu, Philip S Yu, and Kai Shu. Beyond tokens: A survey on de-  
 643 coding methods for large language models and large vision-language models. April 2025.  
 644 doi: 10.36227/techrxiv.174495300.03784996/v1. URL <http://dx.doi.org/10.36227/techrxiv.174495300.03784996/v1>.

645

646 Noah Wang, Zy Peng, Haoran Que, Jiaheng Liu, Wangchunshu Zhou, Yuhua Wu, Hongcheng Guo,  
 647 Ruitong Gan, Zehao Ni, Jian Yang, et al. Rolellm: Benchmarking, eliciting, and enhancing  
 648 role-playing abilities of large language models. In *Findings of the Association for Computational  
 649 Linguistics: ACL 2024*, pp. 14743–14777, 2024a.

648 Yubo Wang, Xueguang Ma, Ge Zhang, Yuansheng Ni, Abhranil Chandra, Shiguang Guo, Weiming  
649 Ren, Aaran Arulraj, Xuan He, Ziyan Jiang, et al. Mmlu-pro: A more robust and challenging  
650 multi-task language understanding benchmark. *arXiv preprint arXiv:2406.01574*, 2024b.  
651

652 Yongliang Wu, Yizhou Zhou, Zhou Ziheng, Yingzhe Peng, Xinyu Ye, Xinting Hu, Wenbo Zhu,  
653 Lu Qi, Ming-Hsuan Yang, and Xu Yang. On the generalization of sft: A reinforcement learning  
654 perspective with reward rectification, 2025. URL <https://arxiv.org/abs/2508.05629>.  
655

656 Yang Yue, Zhiqi Chen, Rui Lu, Andrew Zhao, Zhaokai Wang, Shiji Song, and Gao Huang. Does  
657 reinforcement learning really incentivize reasoning capacity in llms beyond the base model? *arXiv  
658 preprint arXiv:2504.13837*, 2025.

659 Jeffrey Zhou, Tianjian Lu, Swaroop Mishra, Siddhartha Brahma, Sujoy Basu, Yi Luan, Denny  
660 Zhou, and Le Hou. Instruction-following evaluation for large language models. *arXiv preprint  
661 arXiv:2311.07911*, 2023.

662

663

664

665

666

667

668

669

670

671

672

673

674

675

676

677

678

679

680

681

682

683

684

685

686

687

688

689

690

691

692

693

694

695

696

697

698

699

700

701

702 CONTENTS OF THE PAPER  
703

704	<b>1</b>	
705	<b>1</b>	
706	<b>2</b>	
707	2.1 Training Strategy . . . . .	2
708	2.2 Inference: Dynamic Decoding . . . . .	4
709	<b>4</b>	
710	3.1 Experimental Setup . . . . .	5
711	3.2 Main Results . . . . .	5
712	3.2.1 Performance . . . . .	5
713	3.2.2 Efficiency . . . . .	9
714	3.3 Emergent Control of Decoding via Natural Language . . . . .	9
715	<b>9</b>	
716	<b>9</b>	
717	<b>10</b>	
718	<b>10</b>	
719	<b>14</b>	
720	<b>14</b>	
721	<b>15</b>	
722	<b>15</b>	
723	<b>16</b>	
724	<b>16</b>	
725	<b>16</b>	
726	<b>18</b>	
727	<b>18</b>	
728	<b>6</b>	
729	<b>EXPERIMENTAL SETUP</b>	

730 **Training.** For the training of all models with our AutoDeco framework, we employed a consistent  
731 hyperparameter configuration to ensure fair comparison. To efficiently manage memory and scale our  
732 experiments, we utilized the DeepSpeed library with the ZeRO Stage 3 optimization. The specific  
733 training settings are detailed below:

734

- 735 • **Training Framework:** DeepSpeed (ZeRO Stage 3) for DeepSeek-R1-Distill-Qwen-7B and  
736 Llama-3.1-Llama-Nemotron-8B-8B-Nano-v1. Megatron for the MoE model Qwen3-30B-A3B-  
737 Instruct-2507, Qwen3-235B-A22B-Thinking-2507, OpenAI-GPT-Oss-20B-Oss-20B, OpenAI-  
738 GPT-Oss-20B-Oss-120B, and DeepSeek-V3.1-Terminus.
- 739 • **Hardware:** 32 GPUs for DeepSeek-V3.1-Terminus, 8 GPUs for the others.
- 740 • **Batch Size:** A per-device batch size of 1 with 4 gradient accumulation steps, resulting in an  
741 effective global batch size of 32.
- 742 • **Optimizer:** AdamW
- 743 • **Learning Rate:**  $5 \times 10^{-6}$ .
- 744 • **Max Token Length:** 16384.
- 745 • **Decay Steepness  $\alpha$ :** 30.

746 For each task, we calculated the Pass@1 through oversampling (16 times). To ensure the results  
747 are solid, we do 8 runs on each experiment with different seeds. For all the tasks, our maximum  
750 generation length is 32768.

751 **Datasets.** Our experimental configuration is detailed as follows:

752

- 753 • **MMLU-Pro:** We used a comprehensive and evenly distributed “lite” subset<sup>3</sup> for evaluation to  
754 ensure a balanced assessment across all subject areas.

755 <sup>3</sup><https://huggingface.co/datasets/koiwave/100MMLUpro>

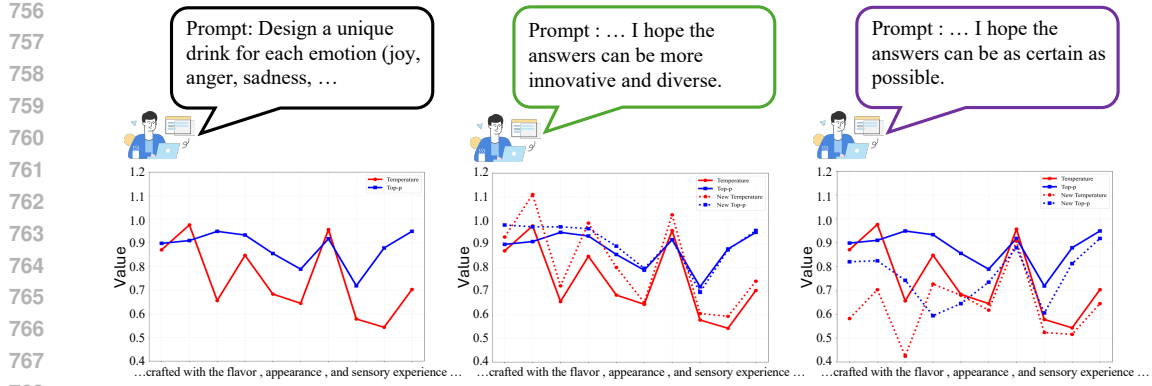


Figure 5: **An Emergent Phenomenon.** This figure shows the token-level  $\hat{T}/\hat{P}$  predictions for the same prompt under three conditions, observed *without* any targeted training. **(Left) Baseline:** The model’s default dynamic  $\hat{T}/\hat{P}$  values. **(Middle) High-Diversity Command:** The model spontaneously elevates its  $\hat{T}/\hat{P}$  predictions. **(Right) Low-Diversity Command:** The model spontaneously suppresses its  $\hat{T}/\hat{P}$  predictions.

Table 5: Quantitative Impact of Diversity Commands on Predicted Decoding Parameters (N=100).

Command	Avg. Temp.	$\Delta$ Temp.	Consistency (T)	Avg. top-p	$\Delta$ top-p	Consistency (P)
Baseline (No Cmd)	0.59	-	-	0.84	-	-
Low Diversity	<b>0.48</b>	↓ <b>0.11</b>	<b>99%</b>	<b>0.75</b>	↓ <b>0.09</b>	<b>99%</b>
High Diversity	<b>0.66</b>	↑ <b>0.07</b>	<b>90%</b>	<b>0.89</b>	↑ <b>0.05</b>	<b>96%</b>

- **LiveCodeBench:** The V6 version of the dataset was used. The evaluation window for this benchmark was initiated on September 1, 2023, and included all subsequent data.
- **Others:** All the others selected datasets were processed using their full sets.

## 7 IN-DEPTH DISCUSSION ON INSTRUCTION-BASED DECODING CONTROL

The instruction-based decoding control capability is indeed an unexpected yet interesting phenomenon discovered during our experiments.

Figure 5 provides a qualitative demonstration of this capability. On the left, a creative prompt to “Design a unique drink for each emotion” elicits a dynamic but baseline set of temperature and top-p values (solid lines). In the middle panel, when we append the command, “I hope the answers can be more innovative and diverse,” the model’s response is immediate and visible: the predicted T and P values (dotted lines) are consistently elevated above the baseline, effectively “turning up” its own creativity. Conversely, on the right, the command “I hope the answers can be as certain as possible” causes the model to autonomously suppress its T and P predictions, “turning down” its randomness to favor more deterministic outputs. To our knowledge, this is the first demonstration of an LLM directly translating natural language intent for creativity and certainty into its internal sampling parameters on a token-by-token basis.

To verify that this is not an anecdotal result, we conducted a large-scale quantitative analysis. We prepended commands for “high” or “low” diversity to a set of 100 questions and aggregated the results, presented in Table 5. The data confirms the effect is systematic and robust. The “low diversity” command prompted a substantial drop in average temperature from 0.59 to 0.48 with remarkable **99% consistency** across all questions. The “high diversity” command triggered a similarly consistent increase in both temperature and top-p, proving that the model has learned a generalizable mapping from abstract language to its internal generation mechanics.

However, we do not yet have a conclusive understanding of this phenomenon theoretically. We will continue to advance this.

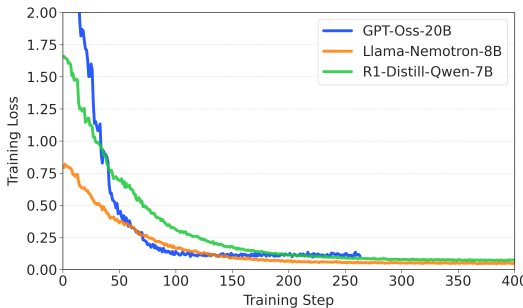


Figure 6: *AutoDeco*’s training curves on all models. Training loss curve across models. The loss converges effectively, indicating resource-friendly training of *AutoDeco*.

Table 6: Pass@16 accuracy on mathematical reasoning benchmarks. Comparing Default Sampling with the *AutoDeco* method.

Model	Method	AIME	BRUMO25	HMMT25	BeyondAIME	Average
Llama-Nemotron-8B	Default Sampling	77.47	82.46	82.46	82.46	81.21
<i>AutoDeco</i> (Ours)		<b>80.31</b>	<b>84.18</b>	<b>84.18</b>	<b>84.18</b>	<b>83.21</b>
R1-Distill-Qwen-7B	Default Sampling	71.16	74.83	49.79	53.16	62.24
<i>AutoDeco</i> (Ours)		<b>73.86</b>	<b>79.03</b>	<b>57.48</b>	<b>54.54</b>	<b>66.23</b>
Qwen3-30B-Instruct	Default Sampling	87.53	87.47	<b>64.86</b>	<b>69.32</b>	77.30
<i>AutoDeco</i> (Ours)		<b>88.44</b>	<b>89.11</b>	64.48	69.08	<b>77.78</b>
Qwen3-235B-Thinking	Default Sampling	91.25	92.84	82.81	68.38	83.82
<i>AutoDeco</i> (Ours)		<b>91.82</b>	<b>94.72</b>	<b>83.41</b>	<b>68.93</b>	<b>84.72</b>
OpenAI-GPT-OSS-20B	Default Sampling	91.42	92.27	74.91	<b>77.02</b>	83.91
<i>AutoDeco</i> (Ours)		<b>91.48</b>	<b>92.82</b>	<b>81.91</b>	75.60	<b>85.45</b>

## 8 SUPPLEMENTARY DISCUSSION OF EFFICIENCY

**Training Efficiency.** Given *AutoDeco*’s superior decoding performance and minimal deployment overhead, a natural question arises: What is the cost of endowing a language model with this adaptive decoding capability? Remarkably, the answer is negligible. *AutoDeco* is a resource-efficient, general-purpose solution for adaptive decoding optimization. Our experiments reveal two key practical advantages:

- Label-free supervision: *AutoDeco* eliminates the need to pre-compute or invoke any external optimization modules to generate supervision signals (e.g., temperature or top-p labels) for fine-tuning.
- Data efficiency: We show the training curves of all models in Figure 6, and *AutoDeco* achieves strong performance within about only 6K training samples and 400 steps, making it effortlessly be integrated into any pre-trained LLMs.

## 9 SUPPLEMENTARY EXPERIMENTAL RESULTS

**Adaptability to Stability and Creativity.** We selected the eight benchmarks in the main paper primarily because they are widely recognized, standard benchmarks that are frequently featured in the technical reports of leading LLMs. Furthermore, *AutoDeco* has proven effective in common open-ended generation scenarios like role-playing, enabling us to eliminate manual decoding without performance degradation. To demonstrate this, we also evaluated *AutoDeco*’s effectiveness on the RoleLLM (Wang et al., 2024a) benchmark:

- Model: Qwen3-30B-A3B-Instruct-2507.

864  
865  
866  
Table 7: Pass@32 accuracy on mathematical reasoning benchmarks. Comparing Default Sampling  
with the *AutoDeco* method.

867 Model	868 Method	869 AIME	870 BRUMO25	871 HMMT25	872 BeyondAIME	873 Average
874 Llama-Nemotron-8B	875 Default Sampling	876 80.65	877 85.74	878 85.74	879 85.74	880 84.47
	881 <i>AutoDeco</i> (Ours)	882 <b>84.02</b>	883 <b>87.24</b>	884 <b>87.24</b>	885 <b>87.24</b>	886 <b>86.44</b>
887 R1-Distill-Qwen-7B	888 Default Sampling	889 73.69	890 77.57	891 57.74	892 58.44	893 66.86
	894 <i>AutoDeco</i> (Ours)	895 <b>76.89</b>	896 <b>81.03</b>	897 <b>65.58</b>	898 <b>59.65</b>	899 <b>70.79</b>
900 Qwen3-30B-Instruct	901 Default Sampling	902 89.07	903 89.96	904 <b>68.41</b>	905 <b>73.65</b>	906 <b>80.27</b>
	907 <i>AutoDeco</i> (Ours)	908 <b>90.00</b>	909 <b>91.68</b>	910 66.09	911 73.02	912 80.20
913 Qwen3-235B-Thinking	914 Default Sampling	915 91.65	916 94.04	917 <b>86.09</b>	918 <b>70.67</b>	919 <b>86.22</b>
	920 <i>AutoDeco</i> (Ours)	921 <b>92.08</b>	922 <b>96.66</b>	923 85.45	924 <b>81.03</b>	925 87.08
926 OpenAI-GPT-OSS-20B	927 Default Sampling	928 92.91	929 93.84	930 80.54	931 <b>93.55</b>	932 <b>95.41</b>
	933 <i>AutoDeco</i> (Ours)	934 <b>95.41</b>	935 <b>87.05</b>	936 80.92	937 <b>89.23</b>	938

887  
Table 8: The WinRate of *AutoDeco* / fixed decoding parameters on RoleLLM.

888 WinRate	889 $T = 0, Top - p = 0$	890 $T = 0.7, Top - p = 0.8$	891 $T = 0.8, Top - p = 0.95$	892 $T = 0.9, Top - p = 0.95$
893 <i>AutoDeco</i>	894 <b>54.65</b> / 45.35	895 54.32 / 45.68	896 53.82 / 46.18	897 52.21 / 47.79

898  
Table 9: The average predictions of *AutoDeco* in different tasks.

899 AIME		900 Creative Tasks
901 <i>AutoDeco</i>	902 $\hat{T} = 0.61, \hat{P} = 0.93$	903 $\hat{T} = 1.18, \hat{P} = 0.88$

898  
• Evaluation: We employed the advanced Claude-Sonnet-3.7 to do LLM Judge to compare  
899  
generations using *AutoDeco*’s dynamic predictions against generations using several optimized  
900  
fixed-parameter settings.

901  
As demonstrated in Table 8, *AutoDeco* consistently outperforms all optimized fixed-parameter settings  
902  
in these head-to-head comparisons.

903  
We conducted an additional comparison on Qwen3-235B-A22B-Thinking-2507, between two distinct  
904  
generation regimes: Mathematical Reasoning (which favors relatively high consistency/stability) and  
905  
creative task (which benefits from higher variability/creativity).

906  
• Math Results: Average results of AIME sampling.  
907  
• Creative Tasks: Average results of 20 distinct prompts. (e.g., ”Please write a story about a cat”  
908  
and ”Help me plan a trip to Europe.”)

909  
The average predictions shown in Table 9 demonstrates the ability of *AutoDeco* to adapt to different  
910  
task requirements.

911  
**Pass@k Performance.** With encouraging results, we find that the absolute improvements delivered  
912  
by *AutoDeco* at higher  $k$ -values are consistent with, and at times even slightly greater than, those  
913  
observed at pass@1.

914  
It is important to note that for any given model, pass@ $k$  accuracy is inherently much higher than  
915  
pass@1 accuracy. Consequently, it is obvious that securing absolute performance gains becomes  
916  
substantially more difficult, and a similar absolute improvement at pass@64 translates to a much  
917  
larger relative error reduction, compared to pass@1. For example, on the OpenAI-GPT-OSS-20B  
918  
model, we observe that the performance gains from *AutoDeco* are consistent across different  $k$  values  
919  
in pass@ $k$  evaluations. More importantly, this consistent absolute gain translates to a significantly  
920  
larger impact in higher-accuracy (when  $k$  is large) scenarios. The relative error reduction dramatically  
921  
increases from **3.5%** at pass@1 to **18.1%** at pass@64. This demonstrates that as the task becomes  
922  
easier for the baseline model (i.e., the error rate decreases at high  $k$ ), the performance gains from our  
923  
method become even more significant.

918 Table 10: Pass@1 accuracy on Synthetic-100. *AutoDeco* consistently outperforms both Greedy  
 919 Search and Default Sampling methods  
 920

921 Model	922 Greedy Search	923 Default Sampling	924 <i>AutoDeco (Ours)</i>
925 DeepSeek-671B	926 56.94	927 57.76	<b>928 58.47</b>
929 DeepSeek-685B (with MTP)	930 57.12	931 57.89	<b>932 58.40</b>

926 Table 11: Pass@1 accuracy on mathematical reasoning benchmarks. *AutoDeco* consistently outper-  
 927 forms both greedy Search and Default Sampling methods across various models.  
 928

929 Model	930 Method	931 AIME	932 BRUMO25	933 HMMT25	934 BeyondAIME	935 Average
930 Llama-Nemotron-8B	Greedy Search	51.67	56.67	26.67	<b>35.00</b>	42.50
	Default Sampling	50.84±1.44	57.89±1.46	29.82±1.60	31.82±0.40	42.59
	<i>AutoDeco</i> (Ours)	<b>55.43±1.22</b>	<b>60.60±0.98</b>	<b>33.98±1.14</b>	34.19±0.65	<b>46.05</b>
933 R1-Distill-Qwen-7B	Greedy Search	38.33	43.33	16.67	24.00	30.58
	Default Sampling	43.49±1.38	49.01±1.10	22.32±0.83	24.21±0.79	34.76
	<i>AutoDeco</i> (Ours)	<b>47.03±1.12</b>	<b>51.64±1.05</b>	<b>24.14±0.39</b>	<b>26.65±0.49</b>	<b>37.37</b>
936 Qwen3-30B-Instruct	Greedy Search	65.00	63.33	36.67	44.00	52.25
	Default Sampling	67.92±1.36	66.02±1.11	<b>43.88±1.28</b>	46.38±0.47	56.05
	<i>AutoDeco</i> (Ours)	<b>68.46±0.76</b>	<b>67.21±0.87</b>	43.73±1.26	<b>46.75±0.18</b>	<b>56.54</b>
938 Qwen3-235B-Thinking	Greedy Search	80.00	79.92	63.33	51.00	68.56
	Default Sampling	80.76±0.43	79.32±0.79	61.95±0.94	49.15±0.33	67.80
	<i>AutoDeco</i> (Ours)	<b>82.79±0.72</b>	<b>80.96±1.05</b>	<b>64.17±0.91</b>	<b>51.19±0.47</b>	<b>69.78</b>
941 OpenAI-GPT-OSS-20B	Greedy Search	56.67	66.67	<b>46.67</b>	36.00	51.50
	Default Sampling	69.61±1.32	67.03±1.12	44.24±2.28	45.69±0.13	56.64
	<i>AutoDeco</i> (Ours)	<b>72.33±1.20</b>	<b>68.25±0.58</b>	46.21±1.08	<b>45.72±0.44</b>	<b>58.13</b>
943 OpenAI-GPT-OSS-120B	Greedy Search	78.33	60.00	53.33	39.00	57.67
	Default Sampling	78.33±0.72	62.72±0.45	<b>53.45±0.28</b>	44.12±0.14	59.66
	<i>AutoDeco</i> (Ours)	<b>78.52±0.50</b>	<b>63.49±0.47</b>	52.58±0.55	<b>44.43±0.20</b>	<b>59.76</b>

947 **DeepSeek-V3.1-Terminus.** The performance gains achieved on production-level models are our  
 948 main focus. We have also conducted performance evaluations on industrial-grade SOTA large models  
 949 such as DeepSeek-V3.1-Terminus-671B (DeepSeek-AI, 2024).

950 Due to the deployment and sampling pressure of the ultra-large thinking model, we combined all the  
 951 evaluated benchmarks on an average basis and created a tiny synthetic benchmark consisting of 100  
 952 evaluation questions (named Synthetic-100) for evaluating *AutoDeco*.

953 Our method is fully compatible and integrates seamlessly with speculative decoding mechanisms.  
 954 Taking MTP as an example, it is fundamentally still of the form of autoregression. Sampling  
 955 parameters such as Temperature and Top-p are widely and continuously employed within it to control  
 956 the diversity and quality of the final accepted tokens.

957 To empirically confirm this seamless integration, we conducted a MTP experiment on the advanced  
 958 LLM DeepSeek-V3.1-Terminus and demonstrate the superiority of *AutoDeco* in Table 10. It proves  
 959 that using *AutoDeco* will not disrupt the MTP process of the model. Critically, we find that the  
 960 sampling parameters temperature and top-p are still of vital importance and do not diminish as the  
 961 size and capability of the model increase. *AutoDeco* can help users achieve the best performance with  
 962 the least effort.

## 964 10 DECLARATION OF LLM USAGE

966 The LLM is used only for writing, editing, or formatting purposes and does not impact the core  
 967 methodology, scientific rigorousness, or originality of the research.  
 968

972  
 973  
 974  
 975  
 976  
 977  
 978  
 979  
 980  
 981  
 982  
 983  
 984  
 985  
 986  
 987  
 988  
 989

990  
 991 Table 12: Pass@1 accuracy on general-domain benchmarks. *AutoDeco* shows exciting generalization  
 992 performance across General QA, Code Generation, and Instruction Following tasks.

Model	Method	GPQA-Diamond	MMLU-Pro	LiveCodeBenchV6	IFEval	Average
Llama-Nemotron-8B	Greedy Search	<b>51.01</b>	52.00	19.17	<b>71.53</b>	48.43
	Default Sampling	44.93	54.00	21.22	65.25	46.35
	<i>AutoDeco</i> (Ours)	50.52	<b>55.64</b>	<b>21.68</b>	71.02	<b>49.72</b>
R1-Distill-Qwen-7B	Greedy Search	37.87	47.20	49.13	32.90	39.32
	Default Sampling	47.41	47.65	53.00	32.35	42.47
	<i>AutoDeco</i> (Ours)	<b>48.91</b>	<b>50.75</b>	<b>53.14</b>	<b>33.90</b>	<b>46.88</b>
Qwen3-30B-A3B-Instruct-2507	Greedy Search	65.86	78.00	47.75	<b>83.73</b>	68.84
	Default Sampling	69.82	76.25	48.52	81.52	69.03
	<i>AutoDeco</i> (Ours)	<b>69.96</b>	<b>78.38</b>	<b>49.80</b>	82.81	<b>70.24</b>
Qwen3-235B-Thinking	Greedy Search	77.78	<b>81.00</b>	77.25	31.98	67.00
	Default Sampling	80.81	80.33	77.47	31.61	67.56
	<i>AutoDeco</i> (Ours)	<b>81.13</b>	79.20	<b>78.10</b>	<b>32.90</b>	<b>67.83</b>
OpenAI-GPT-OSS-20B	Greedy Search	59.60	67.00	69.69	29.94	56.56
	Default Sampling	65.67	68.00	70.15	30.68	58.63
	<i>AutoDeco</i> (Ours)	<b>66.48</b>	<b>69.12</b>	<b>71.25</b>	<b>30.84</b>	<b>59.42</b>
OpenAI-GPT-OSS-120B	Greedy Search	<b>71.21</b>	75.00	73.93	32.72	63.22
	Default Sampling	70.20	76.00	74.19	32.53	63.23
	<i>AutoDeco</i> (Ours)	70.24	<b>76.50</b>	<b>74.30</b>	<b>32.90</b>	<b>63.49</b>

1008  
 1009  
 1010  
 1011  
 1012  
 1013  
 1014  
 1015  
 1016  
 1017  
 1018  
 1019  
 1020  
 1021  
 1022  
 1023  
 1024  
 1025